Acta Microscópica, Vol. 1, Nº 2, November 1992, pp 63-83

The Substructure of the backbone of the thick filament from Tarantula muscle

José Reinaldo Guerrero and Raúl Padrón
Laboratorio de Biología Estructural, Instituto Venezolano de Investigaciones Científicas (IVIC), Apdo. 21827, Caracas 1020A, VENEZUELA.

ABSTRACT

Ultrathin transverse sections of the Flexor Metatarsis Longus muscle of the leg of tarantula **Avicularia avicularia** were studied by electron microscopy in order to dermine the internal structure of their thick filaments. Muscles were chemically demembranated, fixed with glutaraldehyde in relaxing solution in the presence of 0.2 or 2% tannic acid, and then processed following standard electron microscopical methods. We found that in the crossbridge region the filaments present a substructure which consist of a central core of 2.8 nm diameter and 3 concentric rings (I,II and III) which are 3.3; 3.3 and 3.9 nm thick respectively. From geometric considerations and the myosin/paramyosin molar ratio we conclude that either the core is composed of a protein which is different than myosin or paramyosin, or it is hollow. Ring I could be formed by 4 features of 2 paramyosin molecules each one. Rings II and III could have 24 features form by 2 myosin tails each one. so the thick filament will have transversally a total of 48 myosin molecules and 8 paramyosin molecules. We propose a model for the axial arrangement of myosin molecules which relates the described backbone substructure to the arrangement of myosin heads on the surface of the thick filaments found from the three-dimensional reconstruction of negatively stained tarantula thick filaments.

KEY WORDS:

myosin, electron microscopy, tarantula, striated muscle, thick filament, backbone.

INTRODUCTION

Thick filaments of striated muscle are formed by polymerization of myosin molecules, whose heads protrude from the surface of the filament to form a helical array, and whose tails pack to form the backbone of the filament [1]. The helical array of heads has been extensively studied by X-ray diffraction and electron microscopy (EM) [2-7]. For tarantula, this helical array is known to 5 nm resolution; both heads have been resolved in a 3D reconstruction obtained from negatively stained, isolated thick filaments [4-6]. In relaxing conditions the heads are arranged with four-fold symmetry [8] in four coaxial, right-handed helices. Four double heads (a"crown") protrude perpendicular to the filament axis every 14.5 nm, with a helix repeat of 43.5 nm. These helices have also been directly visualized in the sarcomere by rapid freezing and freeze substitution [9-11]. From very thin transverse sections of such rapidly frozen muscle the rotational symmetry is confirmed to be fourfold [12].

Despite the wealth of information about the helical arrangement of myosin heads, relatively little is known about the structure of the backbone [13-15]. In low ionic strength, thick filaments fray into subfilaments, the number of subfilaments depending on the species (3 for vertebrate muscle [16-20]; 5-7 for scallop [21] and 4 for tarantula [18-20]). X-ray diffraction of vertebrate [22], crustacean [15], and arthropod [23] muscle suggests that the backbone is formed by 4 nm diameter subfilaments. In EM, the presence of thick filament substructure seen in transverse sections has been reported for different species [24-30]; and 4 nm axial features have been seen in negatively stained thick filaments of tarantula muscle [31]. However, the precise backbone structure has not been solved.

In this paper, we examine the backbone structure of thick filaments from tarantula. We

selected tarantula because the arrangement of myosin heads is known, providing a known geometry on the surface from which to deduce the backbone packing. Tarantula thick filaments are longer (4.2 μm) and thicker (25 nm) than vertebrate thick filaments. They contain a paramyosin core surrounded by myosin in a molar ration of 0.31 [8]. We have used tannic acid/glutaraldehyde fixation [32,33] to obtain improved preservation of the backbone substructure. Preliminary results have been published elsewhere [34-38].

MATERIAL AND METHODS

Solutions: For **spider Ringer** we used the physiological solution determined for the tarantula ***Euripelma californium*** [39], which contained the following (in mM): 190 NaCl, 2 KCl, 4 $MgCl_2$, 4 $CaCl_2$, 1 Na_2HPO_4; pH 7.8 (osmolarity 370 mOsm/Kg). **Demembranating solution** contained (in mM): 100 NaCl, 8 $MgCl_2$, 5 EGTA, 10 Na_2HPO_4, 3 NaN_3, 1 dithiothreitol, 5 ATP, and 0.1% (w/v) saponin; pH 7.0. **Relaxing solution** was the same as the demembranating solution but without the saponin. Rigor solution lacked both saponin and ATP (modified from [40-42]).

Dissections: Specimens were the Flexor Metatarsus Longus (FML) striated muscle from the legs of the tarantula ***Avicularia avicularia*** (kindly classified by Dr. Sylvia Lucas, Instituto Butatan, Sao Paulo, Brasil). Tarantulas collected at San José de Guaribe were kept in a terrarium. Before dissection tarantulas were held at 4° C for 1 hour, then the legs were removed and the muscle dissected, removing the cuticle and adjacent muscles, but leaving the tendons intact and connected to their respective joints. Muscles were mounted in a plastic chamber [43] between two mylar windows and bathed in spider Ringer. Sarcomere length was measured by laser diffraction and adjusted to 6.5-7.5 μm. The chamber permitted us to change the solutions that bathed the muscle [43]. For the relaxed and rigor specimens, muscles were skinned in the relaxed state by changing to the demembranating solution, and continuously agitating (60 rev/min) the chamber for 2 hours at 4° C.

EM processing: Intact specimens were fixed in the chamber with 2.5% glutaraldehyde in spider Ringer (pH 7.0) for 1 hour at 4° C. Skinned specimens were fixed in the chamber with 2.5% Glutaraldehyde and 2 or 0.2% tannic acid (Mallinckrod #1764, lot RJJD, kindly donated by Dr. Roger Craig) in the relaxing or rigor solutions. Tannic acid solutions were prepared just before use because they precipitated with time. Glutaraldehyde was added last, adjusting the pH to 7.0 with NaOH. Muscles were then removed from the chamber and post-fixed with 1% $Os0_4$ for 90 min, stained *en bloc* with 1% uranyl acetate for 1 hour, dehydrated with ethanol (increasing from 50 to 100%), treated with propylene oxide, and embedded with LX-112 resin in the standard way. Blocks were cut on an IVIC diamond knife (Centro Tecnologico, IVIC, Apdo 21827, Caracas 1020-A, VENEZUELA) using a Sorval MT2-B ultramicrotome. Sections were gold to gray in color (<60 nm). Section thickness was verified with a simple method which we developed [44]. Sections were collected on uncoated, 400 or 1000 mesh copper grids. Sections were stained with 6% uranly acetate for 10-20 minutes and then with Reynold's lead stain for 3-5 minutes. Sections were examined in a Hitachi H-500 EM, operated on high resolution mode at 100 KV. Electron micrographs were obtained using Kodak film #4489, developed D-19 (diluted 1:2). Magnifications were calibrated for each microscope session by taking micrographs of a tropomyosin paracrystal, which has a 39.5 nm periodicity [45]. Measurements of the micrographs were made using an ocular micrometer.

RESULTS

Length of thick filaments of FML muscle of **Avicularia avicularia** was determined from longitudinal sections to be 4200 ± 63 nm (mean ± SEM [standard error of the mean], n=18). This agrees with figures obtained for the same species (4000 nm, Rodríguez, personal communication) and other species (4200 nm for ***Eurypelma sp.*** [8]; and 4000-5000 nm for ***Brachypelma sp,*** [6])

Intact muscle: Figure 1 a shows a typical longitudinal section of intact ***Avicularia avicularia*** FML muscle with the characteristic A, I and Z bands. In these muscles it is not easy to locate the H-zone, the M band or the M-bridges. The Z band is not straight and the thick filaments are not in register. Figure 1 b shows a ultrathin (gray, about 30 nm) transverse section of intact FML muscle in which the thick filaments mostly show a solid section, but sometimes show hollow cores, depending of the axial position of sectioning. Figure 1 b show filaments sectioned at

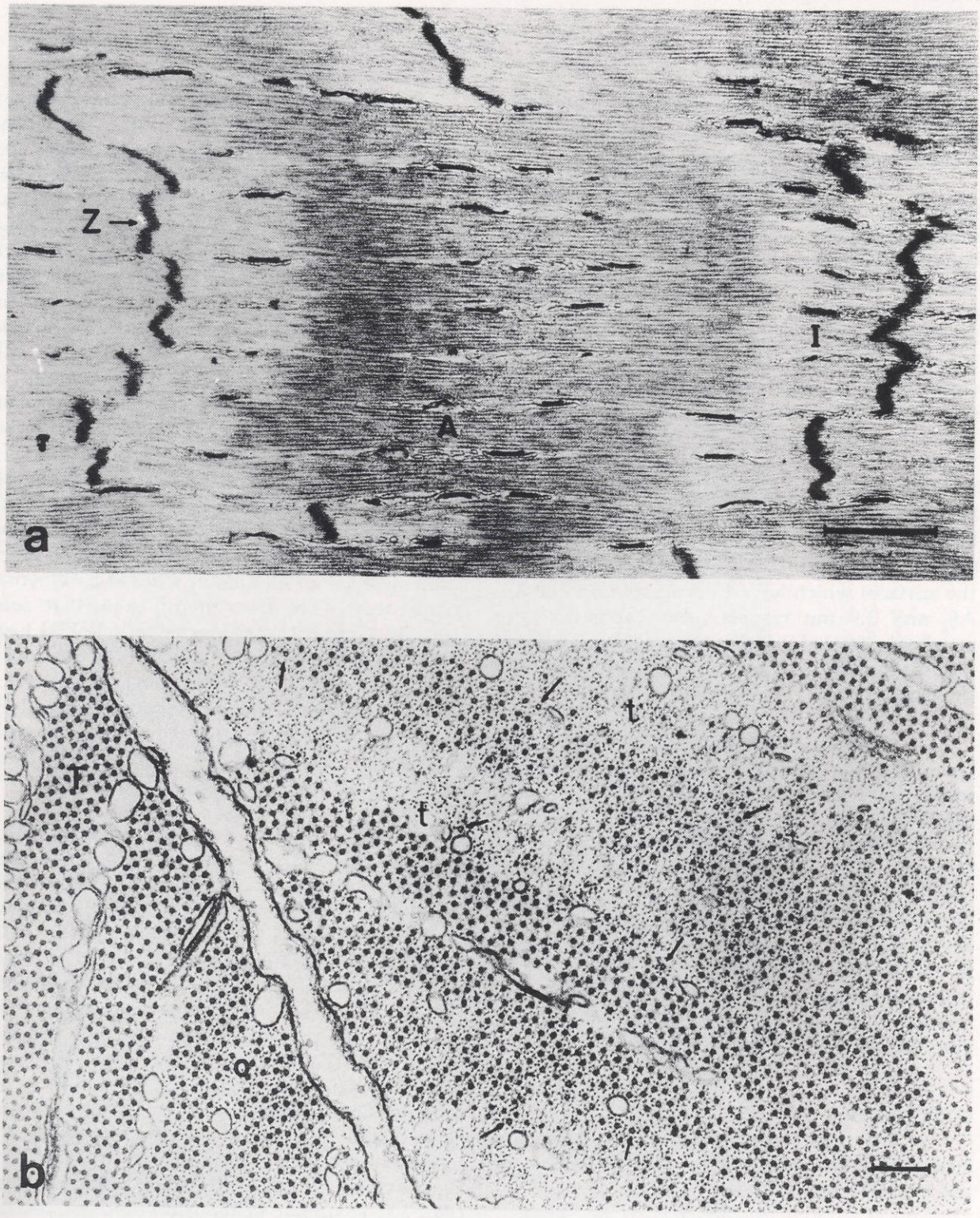

Figure 1. Electron micrograph of sections of intact Flexor Metatarsus Longus (FML) striated muscle of the leg of the tarantula *Avicularia avicularia*, slightly stretched. **(a)** Longitudinal section. **A:** A-band; I: I-band and Z: Z band. Section was gold to gray. Sarcomer length 6.5 - 7.5 µm. Bar: 1 µm. **(b)** Transverse section. **t:** region of the sarcomer close to the Z band showing only thin filaments; O: region of the sarcomer in which there is overlapping of thin and thick filaments; T: region of the sarcomer in which there only thick filaments. The arrows point to thick filaments which are apparently hollow. Ultrathin sections were between silver and gray. Bar: 200 nm.

the H-zone, thick and thin filament overlapping region and thick filament tips. Thick filaments sectioned of the tip show a hollow clear core.

Tannic acid treated muscles: Ultrathin transverse sections of the thick filaments of demembranated FML muscles in relaxing conditions treated with 0.2% tannic acid show dark and clear internal features (Fig. 2). Figure 3 a-f shows a gallery of micrographs of ultrathin sections of thick filaments. The central core is usually either dark (Fig. 3 b-d, f) but sometimes clear (Fig. 3 e), and is surrounded by two and sometimes three concentric rings formed by a number of clear features, and by dark features. Thick filament diameter, in the cross-bridge region, is 24.6 ± 0.2 nm (mean ± SEM, n=131). Dark central core is about 2.8 nm in diameter, surrounded by 2, and sometimes 3, concentric rings of clear features (labeled I, II and III, from the center to the surface) which have thicknesses of about 3.3, 3.8, and 3.9 nm respectively (Table I). Rigor specimens treated with tannic acid show internal organization (Fig. 3 g-1) similar to the relaxed muscle.

Figure 4 shows a series of micrographs taken from the same thick filament at 100 nm step focus from underfocus (Fig. 4 a-b) through overfocus (Fig. 4 d-e). They all show a dark core surrounded by two concentric rings formed by clear features. The most inner ring does not show details, whereas the outer one is formed by well defined features with a diameter similar to the ring thickness. As there are not apparent changes in the images through this focal series on an interval of 400 nm we concluded that the internal features observed in the images studied in this work are not due to a focusing artifact.

DISCUSSION

We report new aspects on the internal structure of the thick filaments revealed by the use of tannic acid fixation.

Difficulties locating H-zone, M band and M-bridges in sarcomer center (Fig. 1 a) are because thick filaments are not aligned axially, M line on this species is not well ordered and does not present M-bridges which are evident in frog [46, 47]. Similar findings were reported for the tarantula **Eurypelma sp.** [8] and **Limulus polifemus** [48]. Lack of M-band in sarcomer have been reported for cockroach [49] and crab [50].

Intact muscle: Thick transverse sections (about 100 nm) show solid thick filaments, without internal detail due to blurring. On ultrathin (gray, 30 nm) sections some internal detail is observed (Fig. 1 b, arrows) like clear centers (of variable diameter) possibly hollow, which we deduce that are the tips of thick filaments because they are located near the thin filaments (I band) and all other thick filaments in the same field are completely dark. Tarantula thick filaments have paramyosin inside [8], giving solid dark features in transverse sections, in agreement with our assumption that paramyosin does not extend to the hollow tip (Fig. 5) and evidences [18 - 20] showing that *Avicularia avicularia* thick filaments only fray on their tips. Probably myosin interacts strongly with paramyosin on the rest of the filament, avoiding total fraying [18 - 20]. On the other hand thick filaments from rat and rabbit without paramyosin content fray easily from the tip to the bare zone [16 - 20]. Crab [51] and lobster muscle [52] have thick filaments which are solid in the bare zone and hollow on the rest of their length. Figure 1 b shows black spots, with less diameter than thick filaments, located near regions of only thin filaments, interpreted as sections of thick filaments just on the their tips. (Fig. 5).

Tannic acid treated muscle: thick filaments (Fig. 2,3) consistently show presence of organized internal structure: a dark central core surrounded by three concentric rings (I, I and III) of clear features (Fig. 4 a-f). Each ring appears to be form by well defined clear rounded features pseudo-negatively stained [32] with dimensions shown on Table I. Core, on most cases, is dark (Fig. 3 a-c, f) and possibly hollow. In few cases it appear clear (Fig. 3 e). We can not conclude if core is solid or hollow. Ring I must be form by paramyosin because it is located internally and rings II and III must be form by myosin as it is located externally [53-55]. Thick filaments in rigor exhibit an organization of concentric rings (Fig. 3 g-1) similar to that observed for relaxed muscle. It is difficult sometimes to observe separately rings II and III, possibly because that these features fuse in a single ring (Fig. 3 g-1).

Proposed models for backbone substructure (crossbridge region): The number of features/ring was not precisely determined because we could not find filaments that show simultaneously all rings. Core and rings were interpreted as shown in

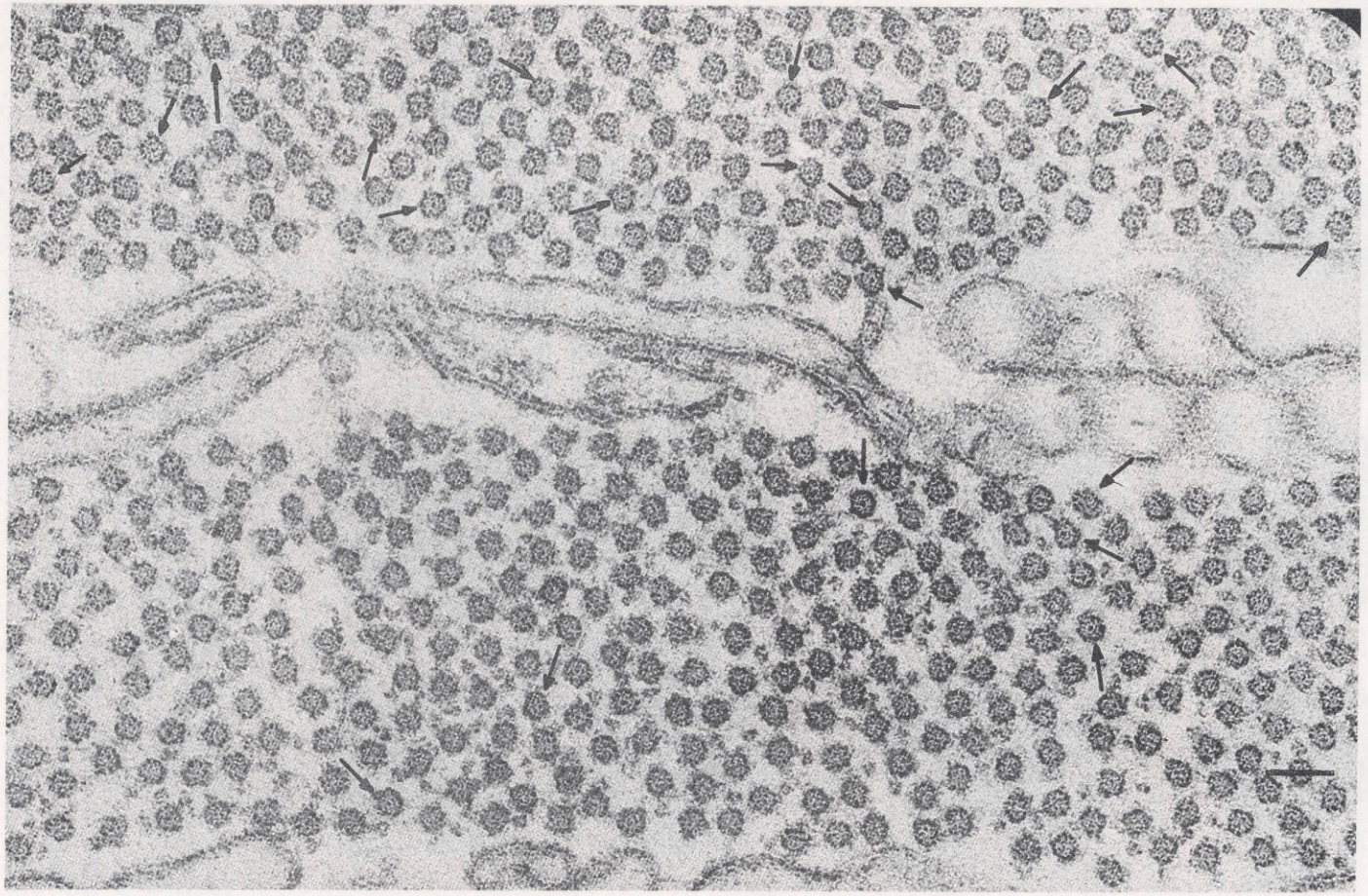

Figure 2. Electron micrograph of ultrathin transverse section (gray; about 30 nm) of relaxed demembranated FML muscle of tarantula leg, treated with 0.2% tannic acid. The thick filaments show consistently well defined internal features (see arrows) Bar 100 nm.

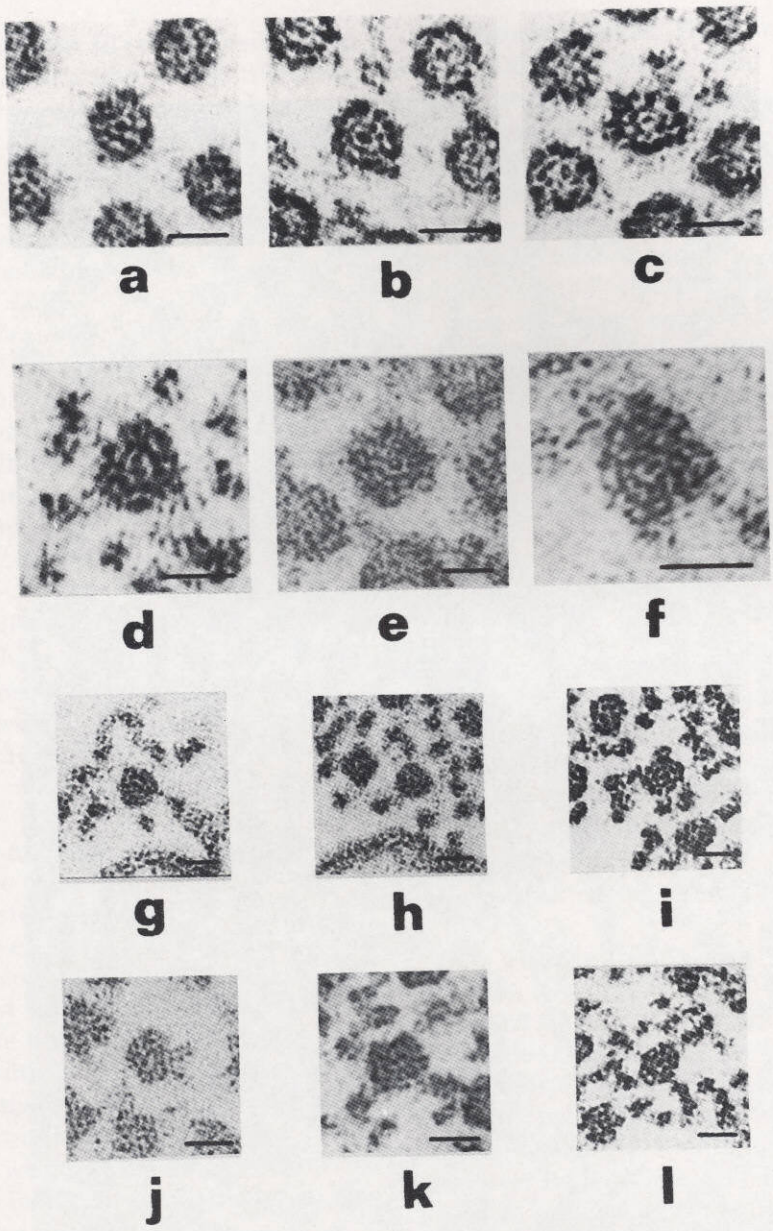

Figure 3. Gallery of electron micrographs of transverse ultrathin sections (30 nm) of slightly stretched demembranated FML muscle, treated with tannic acid. **Relaxed muscle (a-f):** treated with 0.2% (a-c) or 2% (d-f) tannic acid. **Rigor (g-1) muscle:** treated with 0.2% (g-i) or 2% (j-l) tannic acid. Each section shows an organized internal structure which consistently forms a dark central core (sometimes with a hollow center, like e) surrounded by two and sometimes three (see e) rings of dark rounded features. Sections were in the overlap region. Bar: 430 nm.

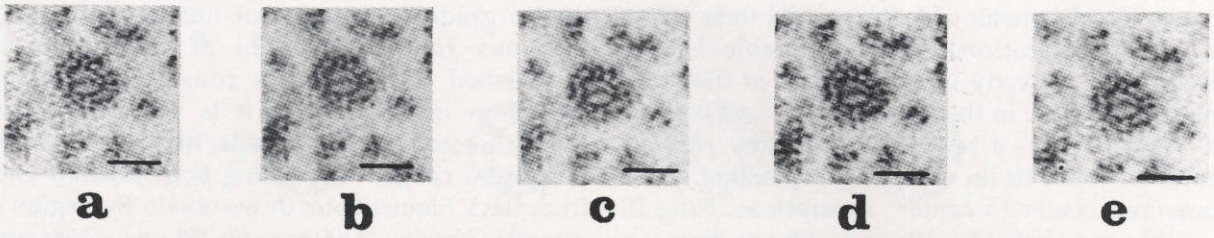

Figure 4. Series of electron micrographs of the same ultrathin section (about 30 nm thick) of a thick filament of relaxed demembranated FML muscle treated with 2% tannic acid, taken at different focus: (a) 200 nm underfocused; (b) 100 nm underfocused; (c) near to focus; (d) 100 nm overfocused and (e) 200 nm overfocused. The internal features does not change through a focal range of 400 nm. Sarcomer length 7.3 μm. Bar: 300 nm.

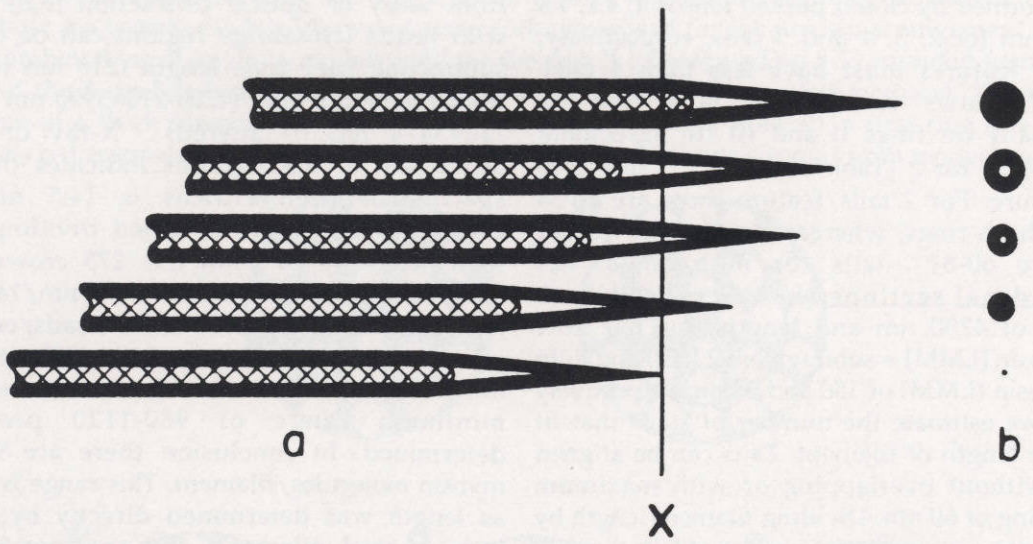

Figure 5. diagram showing the proposed substructure of the tip of a thick filament of tarantula muscle. (a) Diagram to show the hollow tip. The black region represents the myosin region and the crossed region represent the paramyosin core. The tip region, which lacks paramyosin, is hollow. (b) Transverse sections obtained when cutting the tips at different axial positions through the X plane. To simplify, this diagram was not drawn at scale.

Figure 6 a. Diameter of features and their center to center separations shown in Table I were determined directly from the parts of filaments that were visible in the micrographs. Last column of Table I shows a range of how many possible features could fit on each ring depending of the measured center to center separations. Ring III possibly can pack 12 features of 3.9 nm diameter separated by about 5.1 nm or 16 if are completely tight. Rings I and II can possibly pack 4-6 and 8-11 features, respectively. Figure 6 b-d, 6 e-h and 6 i-m show possible models at scale for the core and rings I,II and III, respectively.

a.- Number of myosin tails/filament: (1) Transverse sections: As features have diameters about 3-4 nm (Table I) and myosin tails and paramyosin diameters are 2 nm [56-60], features must be form by more than 1 tail. The diameter of features formed by closed packed tails is 4, 4.2, 4.8 and 5.6 nm for 2, 3, 4 and 5 tails, respectively; therefore features must have less than 4 tails. Table II shows number of tails that fit transversally on rings II and III (in agreement with Table I) for 2 (Table II-A) or 3 (Table II-B) tails/feature. For 2 tails/feature there are 40-54 tails for both rings, whereas for 3 tails/feature there are 60-81 tails for both rings. **(2) Longitudinal sections:** for a length of thick filament of 4200 nm and lengths for tail (low meromyosin [LMM] + subfragment 2 [S2]) and light meromyosin (LMM) of 150 and 90 nm respectively [58, 59] we estimate the number of tails that fit along the length of filament. Tails can be aligned axially without overlapping or with maximum overlapping of 60 nm. Dividing filament length by 90 or 150 nm we can obtain number of tails that can fit along length of filament respectively with and without axial overlapping. Without overlapping filaments must be form by rows of 28 (4200 nm/150 nm) tails. For 60 nm (150nm - 90nm) overlapping filaments would be form by rows of 46 (4200nm/90nm) tails. Total number of tails/filament is found by multiplying 28 or 46 rows by the number of tails that fit transversally. Table III shows total number of tails/filament of 4200 nm length for 2 or 3 tails/feature as indicated in Tables I and II. There is a minimum of 1120 (28x[8+12]x2) tails without axial overlapping and 2 tails/feature; whereas there is a maximum of 3726 (46x[11+16]x3) tails with axial overlapping of 60 nm and 3 tails/feature. So a 4200nm long thick filament must have 1120-3726 tails. Thick filaments present 258 nm tapering at both ends [14] due to gradual reduction of number of myosin. Previous range 1120-3726 of tails must be diminished if tapering is considered. As this reduction is not abrupt it is not possible to calculate total number of tails/filament, but only propose a range. Subtracting both tapered ends from thick filament length we obtain the region of complete packing (4200 nm - (2x258 nm) = 3684 nm). Table III shows total number of tails/filament calculated for 3684 nm length. New minimum is 960 (24x [8+12]x2) tails without axial overlapping and 2 tails/feature; and new maximum is 3240 (40x[11+16]x3) tails with axial overlapping and 3 tails/feature. Thick filament would have minimum number of tails of 960-1120 and maximum of 3240-3726. Table III present 20x8=160 models corresponding to all combinations shown in Figure 6 and Tables I and II. Number of tails can be estimated independently considering evidences from x-ray or optical diffraction [6,8]. Length with heads (crossbrige region) can be obtained subtracting bare zone length (210 nm [6]) from thick filament length (4200-210=3990 nm or 3684-210=3474 nm if tapered). X-ray or optical diffraction of micrographs indicates that axial spacing between crowns is 14.5 nm [6,8]. Crowns/filament are obtained dividing length with heads by 14.5 nm (i.e. 275 crowns (3990 nm/14.5 nm) or 239 crowns (3474 nm/14.5 nm if tapered). As there are 4 double heads/crown [6] we estimate 956 (239x4) or 1100 (275x4) myosin molecules/filament in agreement with the minimum range of 960-1120 previously determined. In conclusion there are 956-1100 myosin molecules/filament. This range is reliable, as length was determined directly by E.M. of isolated thick filaments and spacings by x-ray diffraction or optical diffraction of micrographs. This range, which agrees with the 1046 myosin molecules/filament reported [61] for *Avicularia avicularia*, permits to discard most of models of Table III. Models with axial overlapping in Table III can be discarded because have more than 1600 myosin molecules. We conclude that there can not be no axial overlapping on these thick filaments. Models without axial overlapping with 3 tails/feature can be discarded because they contain more than 1440 myosin molecules. So we can discard all models with 3 tails/feature, remaining possible only models with 2 tails/feature. We discard Table II-B concluding that transversally it is only possible 40-54 rows of tails (Table II-A). Evidences suggest that heads are organized in surface forming 4 coaxial helices

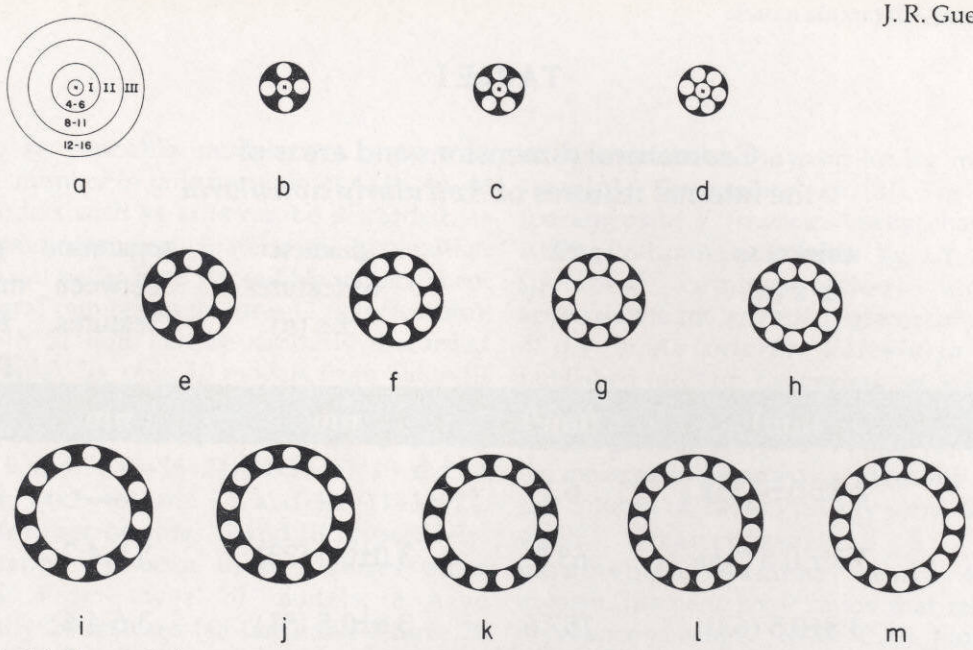

Figure 6. (a) General diagram (drawn at scale) of the transverse section (at crossbridge region) of a thick filament from striated muscle of tarantula, showing the core and 3 concentric circular rings, labeled I, II and III. Diagrams (drawn at same scale) of the three models proposed for the paramyosin arrangement (core and ring I, constituted of 4-6 rounded features) are shown in (b-d). (e-m) show the twenty models (drawn at same scale) proposed for the myosin arrangement which are the combinations of any of 4 models [e-h] for the ring II (constituted by 8-11 rounded features) with any of the 5 models (i-m) for the ring III (constituted by 12-16 rounded features). The transverse section of a thick filament can be formed by the core (solid or hollow), a first ring selected from models b-d; a second ring selected from models e-h and a third ring selected from models j-m.

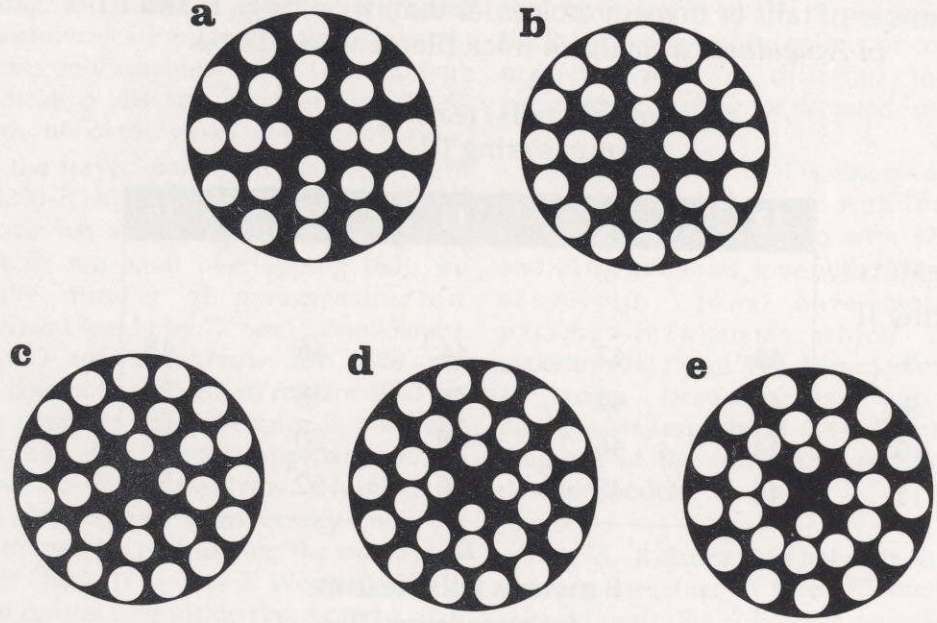

Figure 7. Transverse sections (drawn at scale) of the most feasible models (a-e) indicated in Table VI. All models present a dark core (hollow or constituted by a protein which must be different than paramyosin or myosin) and 4 rounded clear features (constituted of paramyosin) which form the ring I. Only the models that have 48 myosin tails transversally in the rings II and III (b-e) have internal substructure that can be related with the surface array of myosin heads described from the three-dimensional reconstruction of the tarantula muscle thick filament [6]. These features will appear as pseudo-negatively stained features (i.e. clear), as the case for the protofilaments of the microtubules [32]. Model b-e are the most feasible ones for the backbone substructure of *Avicularia avicularia* thick filaments using the criteria established in this work. See text.

TABLE I

Geometrical dimensions and areas of the internal features of *Avicularia avicularia*

	thickness ± s (n)	area	diameter of features ± s (n)	separation between features	possible number of features per ring*
	(nm)	(nm^2)	nm	nm	
core	2.8± 0.5 (35)	6.1	____	____	____
ring I	3.3 ± 0.5 (31)	63.2	3.0±0.3 (23)	3.0-4.2	4-6
ring II	3.8±0.5 (63)	157.6	3.6±0.5 (51)	3.6-4.6	8-11
ring III	3.9±0.4 (40)	248.3	3.8±0.4 (27)	3.9-5.1	12-16

s= standard deviation
n= number of measurements
* Estimated from geometrical considerations [43]

TABLE II

Number of tails of myosin molecules that fit on rings II and III of *Avicularia avicularia* thick filament backbone.

A

2 myosin tails/feature
features/ring III

features/ring II	12	13	14	15	16
8	**40**	42	44	46	48
9	42	44	46	48	50
10	44	46	48	50	52
11	46	48	50	52	**54**

B

3 myosin tails/feature
features/ring III

features/ring II	12	13	14	15	16
8	**60**	63	66	69	72
9	63	66	69	72	75
10	66	69	72	75	78
11	69	72	75	78	**81**

[4-6,8,12]; so probable models are ones with transverse number of tails multiple of 4 (40, 44, 48 or 52). Models with 44 tails can be discarded, as 44/4=11 tails must participate in the generaltion of one coaxial helix; been impossible to pack them in an integral number of features (2 tails/feature). Model with 52 tails can be similarly discarded (52/4=13 tails). So, only 10 models from Table III remain feasible: the ones with 8 and 12 (8+12=20 features; 20x2=40 tails); 8 and 16 (8+16=24; 24x2=48); 9 and 15 (9+15=24; 24x2=48); 10 and 14 (10+14=24; 24x2=48) and 11 and 13 (11+13=24; 24x2=48) features on rings II and III respectively. Discriminating between them requires other evidences. From these 10 models, 8 have transversally 24 features (48 tails) and 2 have 20 features (40 tails). 5 of 10 models correspond to filaments which are 4200 nm long and 5 which are 3684 nm long (tapered).

b.- Number of paramyosin molecules/filament: as done for myosin, we can calculate paramyosin/filament. Evidences indicate that thick filament is hollow at ends (Fig. 1 b, see Fig. 5); so paramyosin core is not present along all filament length. Rodríguez (personal communication) found that tarantula thick filaments only fray near ends (130-190 nm); possibly indicating absence of paramyosin there. Total length of paramyosin core is obtained subtracting the frayed part from filament length (3820 nm (4200-2(130)) or 3940 nm (4200-2(190)). As paramyosin has a rod shape 130 nm long [60] and exhibit 58 nm axial overlapping [60]; we calculate the number of paramyosins/row dividing filament lenght by 72 nm (130nm-58nm). We found 53 molecules/row for 3820 nm paramyosin core or 54 molecules/row for 3940 nm paramyosin core. As the difference is only one paramyosin, and data used is approximate, we will assume 53 molecules/row. Number of paramyosin rows that fit transversally on ring I can be determined by multiplying the number of features (4-6) (Table I) by 2 or 3. We need also to consider that central core inside ring I can be solid or hollow. Results are shown in Table IV. There can be 8-21 rows/filament. Multiplying number of rows by 53 we obtain total number of paramyosin/filament as shown in Table V. So there can be 424-1113 paramyosin/filament.

c.- Biochemical evidences: Using poliacrilamide gel electrophoresis it has been quantitatively determined the relative amounts of paramyosin and myosin for leg muscles of the tarantula ***Eurypelma sp*** [8]. The molar ratio [paramyosin] / [myosin heavy chain] is 0.31 ± 0.079. Preliminary studies by Dr Nelly Panté (personal communication) indicates an approximate molar ratio [paramyosin] / [myosin] of 0.4 for ***Avicularia avicularia*** near to the published ratio for ***Eurypelma sp.*** We will use for following calculations the more precise published ratio of 0.31. From Tables III and V we determined the molar ratio paramyosin/myosin P/M shown in last column of Table VI. Only some of the models with (transversally) 8 rows of paramyosin/filament and 424 paramyosin/filament have ratios that fall inside the experimental range (0.23 - 0.39). Molar ratios are greater for other number of rows/filament. So, all cases in Table IV with 3 paramyosin/feature are discarded. Therefore features must be form (transversally) by 2 paramyosins (or paramyosin rows). From Table IV we also discard models which transversally have more than 8 rows/filament, including models with 2 molecules/feature. From Table IV the only feasible models are the ones with hollow core that have transversally 8 paramyosin. Core of thick filament must be hollow or constituted by a protein which is different to myosin or paramyosin; as occur for nematode muscle [62, 63].

From Table VI it is observed that only 5 of the 6 models of filaments with (transversally) 8 paramyosin/filament (two with 4200 nm length and 40 myosin rows, four with 3684 nm length and 48 myosin rows) have molar ratios of paramyosin/myosin which fall in the experimental range. We discarded one model with 40 rows because its molecular ratio paramyosin/myosin is 0.44. Figure 7 show a diagram of the transverse sections of these 5 possible models.

d.- Relationship between the internal and external structure of thick filament: For models with 48 rows (Fig. 7 b-e) we propose a packing of tails to form the backbone that explain the surface organization of heads as found from the 3D reconstruction [6, 8]. The heads protrude on the surface on 12 radial points spaced azimuthally by 30° (360°/12) as shown by arrows on figure 8. On each radial point protrudes the heads from 4 rows. Numbers on Figure 8 indicate axial positions (spaced 14.5 nm) of heads for one turn of one coaxial helix. Number 1 indicates position of first

TABLE III

Number of myosin molecules that fit on a *Avicularia avicularia* thick filament

myosin molecules/filament

		without overlapping		with overlapping	
tails/feature		2	3	2	3
thick filament length (nm)		4200 3684	4200 3684	4200 3684	4200 3684
features/ring ring II	ring III				
8	12	1120 960	1680 1440	1840 1600	2760 2400
8	13	1776 1008	1764 1512	1932 1680	2898 2520
8	14	1232 1056	1848 1584	2024 1760	3036 2640
8	15	1288 1104	1932 1656	2116 1840	3174 2760
8	16	1344 1152	2016 1728	2208 1920	3312 2880
9	12	1176 1008	1764 1512	1932 1680	2898 2520
9	13	1232 1056	1848 1584	2024 1760	3036 2640
9	14	1288 1104	1932 1656	2116 1840	3174 2760
9	15	1344 1152	2016 1728	2208 1920	3312 2880
9	16	1400 1200	2100 1800	2300 2000	3450 3000
10	12	1232 1056	1848 1584	2024 1760	3036 2640
10	13	1288 1104	1932 1656	2116 1840	3174 2760
10	14	1344 1152	2016 1728	2208 1920	3312 2880
10	15	1400 1200	2100 1800	2300 2000	3450 3000
10	16	1456 1248	2184 1872	2392 2080	3588 3120
11	12	1288 1104	1932 1656	2116 1840	3174 2760
11	13	1344 1152	2016 1728	2208 1920	3312 2880
11	14	1400 1200	2100 1800	2300 2000	3450 3000
11	15	1456 1248	2184 1872	2392 2080	3588 3120
11	16	1512 1296	2268 1944	2484 2160	3726 3240

Note: A length of 4200 nm correspond to a complete thick filament,whereas a length of 3684 nm correspond to a tapered one. The number of myosin molecules was calculated aligning them in a row without overlapping, or with a 60 nm overlapping (see text).

TABLE IV

Number of paramyosin molecules that fit transversally on the core and ring I of *Avicularia avicularia* thick filament.

features/Core	features/ring I	paramyosin 2	molecules/feature 3
0 (hollow)	4	8	12
0 (hollow)	5	10	15
0 (hollow)	6	12	18
1 (solid)	4	10	15
1 (solid)	5	12	18
1 (solid)	6	14	21

TABLE V

Number of paramyosin molecules on the core and ring I of *Avicularia avicularia* thick filament.

Paramyosin molecules/ core filament	Paramyosin molecules/ filament
8	424
10	530
12	636
14	742
15	795
16	848
18	954
21	1113

Note: Length of 3829 nm, corrected for tapering

TABLE VI

Molar ratio [Paramyosin] / [Myosin] (P/M) for models of *Avicularia avicularia* tarantula thick filament.

filament length			feat.		paramyosin	paramyosin	molar
M	P	tails section	/ring (I, II)	tails/ feat.	molecules/ section	molecules/ filament	ratio P/M
4200	3820	**40**	**(8, 12)**	1120	8	424	0,37 **a**
4200	3820	40	(8, 12)	1120	10	530	0,47
4200	3940	40	(8, 12)	1120	10	540	0,48
3684	3820	40	(8, 12)	960	8	424	0,44
3684	3820	40	(8, 12)	960	10	530	0,55
3684	3940	40	(8, 12)	960	10	540	0,56
3684	3820	**48**	**(8, 16)**	1152	8	424	0,36 **b**
3684	3820	48	(8, 16)	1152	10	530	0,46
3684	3940	48	(8, 16)	1152	10	540	0,46
3684	3820	**48**	**(9, 15)**	1152	8	424	0,36 **c**
3684	3820	48	(9, 15)	1152	10	530	0,46
3684	3940	48	(9, 15)	1152	10	540	0,46
3684	3820	**48**	**(10, 14)**	1152	8	424	0,36 **d**
3684	3820	48	(10, 14)	1152	10	530	0,46
3684	3940	48	(10, 14)	1152	10	540	0,46
3684	3820	**48**	**(11, 13)**	1152	8	424	0,36 **e**
3684	3820	48	(11, 13)	1152	10	530	0,46
3684	3940	48	(11, 13)	1152	10	540	0,46

Only models a, b, c, d and e have a molar ratio [P/M] within the range 0,23 - 0,39 [8].
M: myosin
P: paramyosin

double heads (on the plane of the paper). Number 2 the second double heads (located on a plane at 14.5 nm over the plane of the paper), and so on. Head number 13 (first of next turn) would be located exactly over the head number 1 but axially displaced by 174 nm (helix long pith). We define as radial group the 4 rows that have heads protruding on the same direction (Fig. 8). Each radial group would be formed by two of the features seen in transverse sections. Radial group 1 would be formed by two of the features seen in transverse sections. Radial group 1 would be formed exclusively by rows whose heads protrude on radial point 1, and so on. Arrangement of heads as indicated forces axial location of tails on each radial group, and also relative position of radial groups. Assuming that tarantula myosin molecules are 150 nm long [59]; then molecules on each row must be separated axially by 24 nm (Fig. 9 a-d). So one head will emerge every 174 nm. As features are formed transversally by two rows (or tails) of myosin then a first alternative is that there must be an axial displacement of 87 nm (174nm/2nm) between molecules of two rows belonging to the same features. In this case there must be an axial displacement (between features) of 43.5 nm (Fig. 9). With this arrangement myosins must emerge axially (on each radial group) every 43.5 nm. From Figure 9 a-b it can be seen that there are axial displacements of 43.5 or 130.5 nm between myosin molecules that belong to features of the same radial group. Synthetic filaments of vertebrate muscle assemble from myosin dimmers, with tails displaced axially by 43.5 nm. From Figure 9 a-b it is clear that there must be close interactions between the tails of adjacent rows that belong to the same feature: molecule a can interact with the molecules b and c. This type of interaction between (equivalent) myosin-myosin S2-LMM could permit that thick filament grows longer that the end of the paramyosin core. Between features it is probable that there is some type of weak or strong interactions. A second possibility is the one shown in Figure 9 c-d. In this case there is an axial displacement of 43.5 nm between molecules of two adjacent rows that belong to the same feature. There is an axial displacement of 87 nm between the two features that belong to the same radial group. There must be 3 interactions (not equivalent) between the tails of 2 adjacent rows on the same feature: a molecule a could interact with molecules b (interaction S2-S2 and (S2-LMM) - LMM) and c (interaction S2-LMM); but in this case there is a bigger interaction range between a and b than between a and c. In this case also there could be some type of interactions between adjacent features. Previous arrangements are also possible for myosin longer than 150 nm (for a 174 nm long myosin there would not be separation on the same row). Dr Nelly Panté (personal communication) found by metal shadowing preliminary evidences that myosin molecules of **Avicularia avicularia** have an approximate length of 160 nm. [64] have determined a length of 170 nm for the myosin muscle (ABRM) of **Mytilus edulis**. To generate 4 coaxial helices, heads belonging to each one must emerge with an azimuthal rotation of 30° (counterclockwise), between adjacent levels, going from bare zone to tip. So, there must be no axial displacement between radial groups at 90° (no axial displacement between radial groups 1, 4, 7 and 10; 2, 5, 8 and 11; 3, 6, 9 and 12); on quadrant II there must be an axial displacement of 14.5 nm between the adjacent radial groups (spaced by 30°) 1, 2 and 2, 3 and of 29 nm between the radial groups 3, 4 and 3, 1; and the last point must occurs also on the other three quadrants (I, III and IV).

If the thick filament have transversally 48 myosin tails and, these molecules are arranged axially in the way shown in Figures 9 a-b ó 9 c-d; then in one filament of 4200 nm they will fit 1152 ((4200 nm/174 nm) x48) molecules. This data agree closely with the Figure of 1046 reported by [61] for thick filaments of same species. The model that transversally have 40 myosin molecules (Fig. 7 a) would have 10 (40/4) rows per helix, and can not be pack in a way that comply with the experimental evidences of optical and x-ray diffraction mentioned before. So we discard that model. In conclusion, the four model shown in Figure 7 that have transversally 48 myosin tails (Fig. 7 b-e) are the most feasible.

e.- proposed model: the model proposed (4 paramyosins/ring I; 48 tails/rings II & III on 8+16, 9+15, 10+14 or 11+13 arrangements) was built at a scale of about $2x10^6$x. Tails and paramyosin were modeled with copper wires coiled forming coil-coiled helices and heads where modeled with plastic bulbs used for Pasteur pipettes. Figure 10 show a lateral view of the extreme of this model with heads emerging on the surface on the way proposed by [6]. It can be seen that the heads have access to the surface generating 4 coaxial right-handed helices that correspond with the oblique tracks observed on negative

stained thick filaments [6]. These tracks are clearly observed in region b (where filament have normal diameter), but are not well defined near tip (region a); because filament diameter gradually decreases by removal of myosin [14] and because helices are more closer. This model permit to predict that it must be more difficult to visualize helices by negatively staining if they are very close. We suggest also that visualization of helices by negative staining depend on the ratio between filament diameter and the number of helices. For tarantula, tracks can be easily observed [6] because diameter permit the separation of 4 helices. It could be more difficult to observe them if these filament have a greater number of helices. Figure 10 show also that there are head-head interactions between heads that belong to adjacent crowns as proposed by [6] and head-backbone interactions [65-66]. These interactions that made myosin heads closer to the filament surface, also made possible to see helices clearly. We could predict that helices could not be seen so clearly in filaments where myosin heads are not close to the surface of the backbone. This model can be built in a way that the myosin molecules generate right-hand or left-hand helices. However left-handed helices have not been observed [6]. It is possible that right-hand helices are spontaneously generated by specific interaction between heads of two myosin isoforms as occurs in nematode muscle [62].

We (Alamo, Guerrero, Crowther & Padrón, in preparation) currently are analyzing by image processing selected images as shown in Figure 2, trying to determine the rotational symmetry of the core and each ring by calculating its power spectrum, and obtaining rotationally filtered images of them; and by averaging thick filaments images after alignment by using cross-

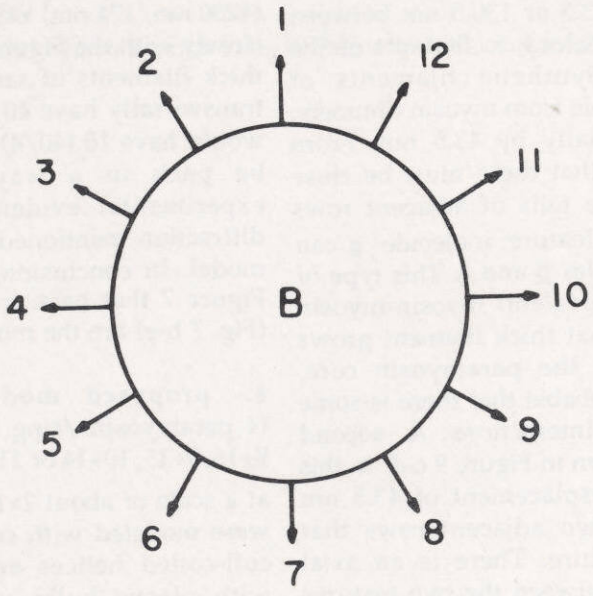

Figure 8. Diagram that represent the radial directions (arrows) and the axial positions (numbers 1-12) of the myosin heads on a turn of one of the coaxial helices of the thick filament of tarantula. Each number give the position of a crown level. Level 1 is located on the plane of the paper. Level 2 is 14.5 nm over the plane of the paper, and so on. In this diagram the bare zone and the tip of the thick filament are located under and over the plane of the paper. B: backbone. See text.

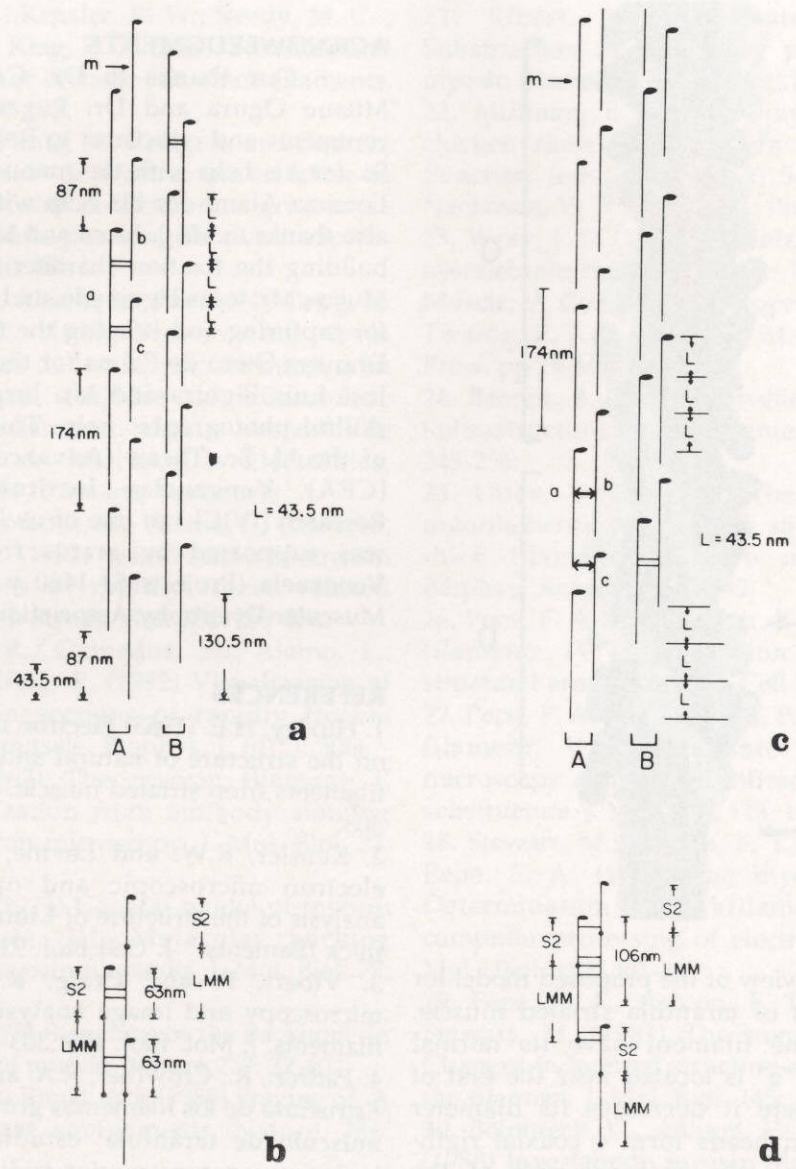

Figure 9. (a) Axial organization proposed for the myosin molecules m on a radial group constituted by two features (A and B) of two rows each one. The two rows of the left feature (A) and right feature (B) form structures which shift axially by 43.5 nm (L). From each radial group two myosin heads emerge to the surface (for simplicity the drawing shows only one head) every 43.5 nm (see Fig. 8). The connections (marked as "=") between the myosin tails of adjacent rows indicate myosin-myosin interactions (for instance, molecule "a" interacts with molecules "b" and "c"). (b) Diagram to show the specific proposed interactions between S2 and LMM ("=") of 63 nm length between the tail of neighboring myosin molecules. (c) Axial organization similar to the one shown in (a) but with an axial shift of 87 nm (2L). The arrows (" <--> ") pointing in opposite directions indicate myosin-myosin interactions between two tails located in adjacent rows (for instance the interaction of molecule "a" with molecules "b" and "c"). (d) Diagram to show the interactions ("-", "=", "≡") between S2-S2, S2-LMM and (S2-LMM) - LMM respectively. Top: tip of filament. Bottom: bare zone.

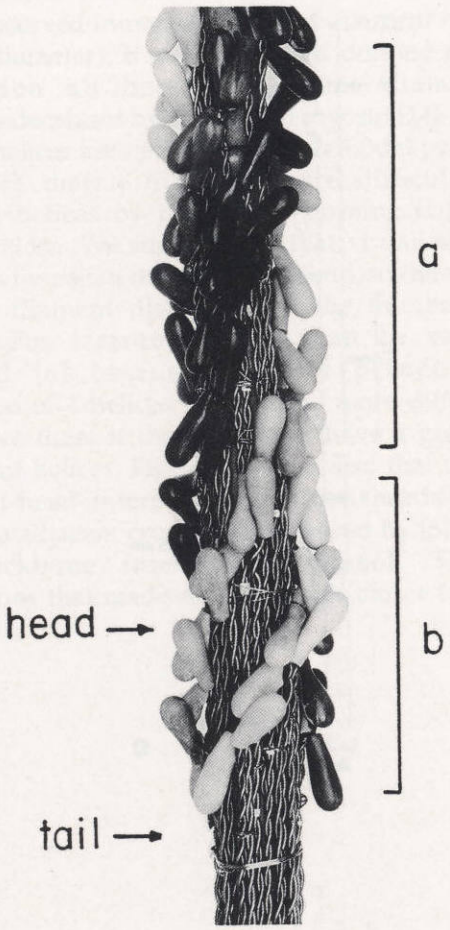

Figure 10. Lateral view of the proposed model for the thick filament of tarantula striated muscle. On region "b" the filament have its normal diameter. Region "a" is located near the end of the filament, where it decreases its diameter gradually. Myosin heads form 4 coaxial rigth-handed helices on the external part of the filament. The myosin tails, which are represented as coil-coiled double helices, pack to form the backbone.

correlation methods developed for similar problems [67 - 69]. We are developing models based on the proposed one for thick filaments of other chelicerate muscles like scorpion or limulus (Guerrero & Padrón, in preparation). Also we are trying to increase preservation of the internal features and to improve resolution by attempting experiments to negatively stain cryosections of rapidly frozen tarantula muscle (Guerrero, Craig & Padrón, in preparation) in order to enhance detail of backbone substructure.

ACKNOWLEDGMENTS

Our thanks to Dr. Carlo Caputo, Dr. Mitsuo Ogura and Dr. Roger Craig for their comments and criticisms; to Robert J. Edwards B. Sc. for his help with the manuscript; and to Lic. Lorenzo Alamo for his help with the figures. We also thanks to Mr. J. Mora and Mr. Pedro Pérez for building the fixation chamber; to Mr. Nehemias Mujica, Mr. Jesús Figueredo, and Mr. Pedro Medina for capturing and keeping the tarantulas; to Mrs. Dhuwya Otero de Palma for the drawings; to Mr. José Luis Bigorra and Mr. Jorge Rivas for their skillful photographic help. This works was part of the M. Sc. Thesis (Advanced Studies Center [CEA], Venezuelan Institute for Scientific Research [IVIC]) of one of us (J.R.G.). This work was supported by grants from CONICIT of Venezuela (Projects S1-1460 y S1-2006) and the Muscular Dystrophy Association (MDA) of U.S.A.

REFERENCES

1. Huxley, H.E. (1963) Electron microscope studies on the structure of natural and synthetic protein filaments from striated muscle. J. Mol. Biol. 7:281-308.

2. Kensler, R.W. and Levine, R.J.C. (1982) An electron microscopic and optical diffraction analysis of the structure of **Limulus** telson muscle thick filaments. J. Cell Biol. 92: 443-451.

3. Vibert, P. and Craig, R. (1983) Electron microscopy and image analysis of scallop thick filaments. J. Mol. Biol. 165: 303-320.

4. Padrón, R., Crowther, R.A. and Craig, R. (1984) Estructura de los filamentos gruesos de miosina de músculo de tarántula: estudio por análisis de imágenes y reconstruccion tridimensional a partir de micrografias electrónicas de mínima dosis. Memorias de las I Jornadas de Microscopía Electrónica, S.V.M.E. pp 28-29., Maracay, Venezuela.

5. Padrón, R., Crowther, R. A. and Craig, R. (1984) Three-dimensional reconstruction of native tarantula muscle thick filaments. Biophys. J. 45: 10a.

6. Crowther, R.A.; Padrón, R. and Craig, R. (1985) Arrangement of the heads of myosin in relaxed thick filaments from tarantula muscle. J. Mol. Biol. 184: 429-439.

7. Kensler, R.W. and Stewart, M. 1986 An structural study of cross-bridge arrangement in the frog thigh muscle thick filament. Biophys. J. 49: 343-351.

8. Levine, R. J. C.; Kensler. R. W.; Reedy, M. C. ; Hofmann, W. and King, H. A. (1983) Structure and paramyosin content of tarantula thick filaments. J. Cell Biol. 97: 186-195.
9. Granados, M., Panté, N., Craig, R. and Padrón, R. (1989) Preservación de la estructura en hélice de las cabezas de miosina en filamentos gruesos de músculo de tarántula por congelamiento rápido. Acta Cient. Ven. 40: 88a.
10. Granados, M., Alamo, L., Panté, N., Craig, R. and Padrón, R. (1990) Preservación de la estructura en hélice de las cabezas de miosina en filamentos gruesos relajados de músculo de tarántula por congelamiento rápido. Memorias de las IV Jornadas de Microscopía Electrónica, S.V.M.E. pp 158-159, Cúmana, Venezuela.
11. Padrón, R., Granados, M., Alamo, L., Guerrero, J. R. and Craig, R. (1992) Visualizatión of myosin helices in sections of rapidly frozen relaxed tarantula muscle. J. Struct. Biol. 108: 269-276.
12. Guerrero, J. R., Granados, M., Alamo, L., Padrón, R. and Craig, R. (1992) Visualización of myosin helices in sections of rapidly frozen, relaxed tarantula muscle. Biophys. J. 61(2): 30la.
13. Pepe, F. (1967) The myosin filament: I. Structural organization from antibody staining observed in electron microscopy. J. Mol. Biol. 27: 203-225.
14. Squire, J. M. (1973) General model of myosin filament structure. III. Molecular packing arrangements in myosin filaments. J. Mol. Biol. 77: 291-323.
15. Wray, J. S. (1979) Structure of the backbone in myosin filaments of muscle. Nature 277: 37-40.
16. Maw, M. C. and Rowe, A. J. (1980) Fraying of A filaments into three subfilaments. Nature, 286: 412-414.
17. Trinick, J. and Cooper, J. (1980) Sequential disassembly of vertebrate muscle thick filaments. J. Mol. Biol. 141: 315-321.
18. Rodríguez, J. and Padrón, R. (1985) Estudio por microscopía electrónica de la subestructura de filamentos gruesos de musculos estriados. Acta Cient. Ven. 36(1): 17.
19. Rodríguez, J. and Padrón, R. (1986) Estudio por microscopía electrónica de la subestructura de los filamentos gruesos de miosina . Memorias de las II Jornadas de Microscopía Electrónica, S.V.M.E. pp 47-48, Caracas, Venezuela.
20. Rodríguez, J. and Padrón, R. (1985) Estudio por microscopía electrónica de la subestructura de los filamentos gruesos de invertebrado. Acta Cient. Ven. 37(1):14
21. Vibert, P. and Castellani, L. (1989) Substructure and accesory proteins in scallop myosin filaments. J. Cell Biol. 109: 539-547.
22. Millman, B. (1979) X-ray diffraction from chicken skeletal muscle. In Motility and Cell Function (eds Pepe, F. A; Sangers, J. W. and Nachmias, V. T.) Academic Press. pp. 351-354.
23. Wray, J. S. (1982) Organization of myosin in invertebrate thick filaments. In Basic Biology of Muscle: A Comparative Approach (ed. by B. M. Twarog, R. J. C. Levine & M. M. Dewey) Raven Press. pp 29-36.
24. Bacceti, B. (1965) Nouvelles observations sur l'ultrastructure du myofilament. J. Ultr. Res. 13: 245-256.
25. Gilev, V. P. (1966) The ultrastructure of myofilaments. II. Further investigation of the thick filaments of crab muscles. Biochim. Biophys. Acta 112: 340-345.
26. Pepe, F. A. and Drucker, B. (1972) The myosin filament: IV. Observation of the internal structural arrangement. J. Cell Biol. 52: 255-260.
27. Pepe, F. A. and Dowben, P. (1977) The myosin filament: V Intermediate voltage electron microscopy and optical diffraction studies of the substructure. J. Mol. Biol. 113: 199-218.
28. Stewart, M.; Ashton, F. T.; Lieberson, R. and Pepe, F. A. (1981) The myosin filament. IX. Determination of subfilament positions by computer processing of electron micrographs. J. Mol. Biol 153: 381-392.
29. Pepe, F. A., Ashton, F. T. Dowben, P. and Stewart, M. (1981) The myosin filament: VII. Changes in internal structure along the length of the filament. J. Mol. Biol. 145: 421-440.
30. Beinbrech, G., Ashton, F. T. and Pepe, F. A. (1988) Invertebrate myosin filament: Subfilament arrangement in wall of tubular filaments of insect flight muscle. J. Mol. Biol. 201: 557-565.
31. Craig, R. and Padrón, R. (1982) Structure of tarantula muscle thick filaments. J. Muscle Res. Cell Motil. 3(4): 487.
32. Tilney, L. G.; Bryan, J.; Bush, J. D.; Fujiwara, K.; Mooseker, M. S.; Murphy, D. B. and Snyder, D. H. (1973) Microtubules: Evidence for 13 protofilaments. J. Cell Biol. 59: 267-275.
33. Simionescu, N. and Simionescu, M. (1976) Galloylglucoses of low molecular weight as mordant in electron microscopy. 70: 622-633.
34. Guerrero, J. R. and Padrón, R. (1985) Determinación por microscopía electrónica de la subestructura del filamento grueso de músculo de tarántula mediante secciones finas. Acta Cient.

Ven. 36(1): 13.
35. Guerrero, J. R. and Padrón, R. (1986) Subestructura de los filamentos gruesos de músculo de tarántula. Memorias de las II Jornadas de Microscopía Electrónica, S.V.M.E., pp 72-73. Caracas, Venezuela.
36. Guerrero, J. R. and Padrón, R. (1986) Estudio por microscopía electrónica de la estructura interna del filamento grueso de músculo de tarántula. Acta Cient. Ven. 37(1): 14.
37 Guerrero, J. R. and Padrón, R. (1989) Subestructura interna del filamento grueso de tarántula. Acta Cient. Ven. 40(1): 88.
38. Guerrero, J. R. and Padrón, R. (1989) Subestructura del filamento grueso de músculo de tarantula. I Iberoamerican Biophysics Congress, pp 180, Sevilla, Spain.
39. Schartau, W. and Leidescher, T. (1983) Composition of the hemolymph of tarantula *Eurypelma californicum*. J. Comp. Physiol. 152: 73-77.
40. Craig, R.; Padrón, R. and Kendrick-Jones, J. (1987) Structural changes accompanying phosphorylation of tarantula muscle myosin filaments. J. Cell Biol. 105: 1319-1327.
41. Vibert, P. and Craig, R. (1985) Structural changes that occur in scallop. J. Cell Biol. 101: 830-837.
42. Padrón, R. and Huxley, H. E. (1984) the effect of the ATP analog AMPPNP on the structure of crossbridges in vertebrate skeletal muscles: X-ray diffraction and mechanical studies. J. Mus. Res. & Cell Motil. 5: 613-655.
43. Guerrero, J. R. Estudio de la subestructura interna del filamento grueso de extremidad de tarántula (*Avicularia avicularia*) y de cangrejo (*Goniopsis croentata*). M. Sc. Thesis. Centro de Estudios Avanzados (CEA), Instituto Venezolano de Investigaciones Científicas (IVIC), Caracas, Venezuela.
44. Guerrero, J. R. and Padrón, R. (1990) Método para la medición del grosor de secciones finas obtenidas por ultramicrotomía. Memorias de las IV Jornadas de Microscopía Electrónica, S.V.M.E. pp 164-165, Cúmana, Venezuela.
45. Caspar, D. L.D., Cohen, C. and Longley, W. (1969) Tropomyosin: crystal structure, polymorphism and molecualr interactions. J. Mol. Biol. 41: 87-107.
46. Knappeis, G. G. and Carlsen, F. (1968) The ultrastructure of M line of skeletal muscle. J. Cell. Biol. 38: 202-211.
47. Luther, P. and Squire, J. M. (1978) Three-dimensional structure of the vertebrate muscle M-region. J. Mol. Biol. 125: 313-324.
48. Dewey, M. M.; Levine, R.J.C. and Colflesh, E. D. (1973) Structure of *Limulus* striated muscle. The contractile apparatus at different sarcomer lengths. J. Cell Biol. 58: 574-593.
49. Hagopian, M. (1966) The myofilament arrangement in the femoral muscle of the cockroach, *Leucopea maderae*. J. Cell Biol. 28: 545-554.
50. Franzini-Armstrong, C. (1970) Natural variability in the length of thin and thick filaments in single fibers from a crab, *Portunus depurator*. J. Cell Sci. 6: 559-592.
51. Reger, J. F. (1967) A comparative study on the striated muscle fibres of the first antenna and the claw muscle of the crab *Pinnixia sp.* J. Ultrast. Res. 20: 72-82.
52. Ashton, F. T.; Beinbrech, G. and Pepe, F. A. (1987) Subfilament organization in myosin filaments of the fast abdominal muscles of the lobster, *Homarus americanus*. Tissue & Cell 19, 51-63.
53. Szent-Györgyi, A. G.; Cohen, C. and Kendrick-Jones, J. (1971) Paramyosin and the Filaments of Molluscan "Catch" Muscles. II. Native Filaments: Isolation and Characterization. J. Mol. Biol. 56, 239-258.
54. Levine, R. J. C.; Dewey, M. M. and De Villafranca, G. W. (1972) Immunohistochemical localization of contractile proteins in *Limulus* striated muscle. J. Cell. Biol. 55: 221-235.
55. Bullard, B.; Hammond, K. S. and Luke, B. M. (1977) The site of paramyosin in insect flight muscle and the presence of an unidentified protein between myosin filaments and Z-line. J. Mol. Biol. 115: 417-440.
56. Hodge, A. J. (1952) A new type of periodic structure obtained by reconstitution of paramyosin from acid solutions. Proc. Natl. Acad. Sci. 38: 850-855.
57. Lowey, S.; Kucera, J. and Holzer, A. (1963) On the structure of the paramyosin molecules. J. Mol. Biol. 7: 234-244.
58. Slayter, H. S. and Lowey, S. (1967) Substructure of the myosin molecule as visualized by electron microscopy. Proc. Natl. Acad. Sci. 58: 1611-1618.
59. Elliot, and Offer, G. (1978) Shape and flexibility of the myosin molecule. J. Mol. Biol. 123: 505-519.
60..Elliot, A. and Lowy, J. (1970) A model for the coarse structure of paramyosin filaments. J. Mol. Biol. 53: 181-203.
61. Sosa, H.; Panté, N. and Padrón, R. (1988) Analisis de la sección ecuatorial del patrón de difracción de rayos-x de musculos estriados de

tarántula en diferentes condiciones experimentales. Acta Cient. Ven. 39: 51-59.

62. Epstein, H. F; Miller III, D. M.; Ortiz, I. and Berliner, G. C. (1985). Myosin and paramyosin are organized about a newly identified core structure. J. Cell Biol. 100: 904-915.

63. Epstein, H. F; Berliner, G. C; Casey, D. L. and Ortiz, I. (1988) Purified thick filaments from the nematode ***Caenorabditis elegans:*** Evidence for multiple proteins associated with core structure. J. Cell Biol. 106: 1985-1995.

64. Castellani, L. and Cohen, C. (1987) Rod phosphorylation favors folding in a catch muscle myosin. Proc. Natl. Acad. Sci. 84: 4058-4062.

65. Padrón, R. and Craig, R. (1989) Disorder induced in non-overlap myosin cross-bridges by loss of adenosine triphosphate. Biophys. J. 56: 927-933.

66. Padrón, R., Panté, N., Sosa, H. and Kendrick-Jones, J. (1991) X-ray diffraction study of the structural changes accompanying phosphorylation of tarantula muscle. J. Muscle Res. Cell Motil. 12: 235-241.

67. Alamo, L., Padrón, R., Craig, R. Hidalgo, C. 1991 Método para la determinación directa de la simetría rotacional de filamentos gruesos de músculo por procesamiento digital de imagenes. Acta Cient. Ven. 42: 59-63.

68. Craig, R., Padrón, R. and Alamo, L. (1991) Direct determination of myosin filament symmetry in scallop striated adductor muscle by rapid freezing and freeze substitution. J. Mol. Biol. 220: 125-132.

69. Alamo, L. , Guerrero, J. R. , Granados, M. , Gherbesi, N. , Craig, R. and Padrón, R. (1992) Direct determination of myosin filament symmetry in tarantula striated muscle by rapid freezing and freeze-substitution. Proceedings of the 10th European Congress on Electron Microscopy, Granada, Spain. Vol. III: pp 53-54.